

Dalton Transactions

Accepted Manuscript



This is an *Accepted Manuscript*, which has been through the Royal Society of Chemistry peer review process and has been accepted for publication.

Accepted Manuscripts are published online shortly after acceptance, before technical editing, formatting and proof reading. Using this free service, authors can make their results available to the community, in citable form, before we publish the edited article. We will replace this *Accepted Manuscript* with the edited and formatted *Advance Article* as soon as it is available.

You can find more information about *Accepted Manuscripts* in the [Information for Authors](#).

Please note that technical editing may introduce minor changes to the text and/or graphics, which may alter content. The journal's standard [Terms & Conditions](#) and the [Ethical guidelines](#) still apply. In no event shall the Royal Society of Chemistry be held responsible for any errors or omissions in this *Accepted Manuscript* or any consequences arising from the use of any information it contains.

A reversible fluorescent-colorimetric imino-pyridyl bis-Schiff base sensor for expeditious detection of Al^{3+} and HSO_3^- in aqueous media

Anupam Ghorai, Jahangir Mondal, Rukmani Chandra and Goutam K Patra*

Department of Chemistry, Guru Ghasidas Vishwavidyalaya, Bilaspur (C.G)

Abstract

A reversible fluorescent-colorimetric imino-pyridyl bis-Schiff base receptor **L** (*N¹E,N⁴E*)-*N¹,N⁴-bis(pyridine-4-ylmethylene)benzene-1,4-diamine* for the detection of both Al^{3+} and HSO_3^- in aqueous medium has been developed. Receptor **L** exhibits an excellent selective fluorescent - colorimetric response toward Al^{3+} . The sensitivity of the fluorescent based assay ($0.903 \mu\text{M}$) for Al^{3+} is far below the limit in the World Health Organization (WHO) guidelines for drinking water ($7.41 \mu\text{M}$). From ^1H NMR data, the Job plot and the ESI-MS spectrum, 1 : 2 stoichiometric complexation between **L** and Al^{3+} has been established. Receptor **L** shows remarkable detection ability in a wide pH range of 4–11 and successfully utilised in the determination of Al^{3+} in aqueous solution of bovine serum albumin protein and HSO_3^- in real food samples. Moreover, **L** shows a highly selective colorimetric response to HSO_3^- by changing its colour from yellow to colorless immediately without any interference from other anions.

*Corresponding Author: Tel.: 91 7587312992, E-mail: patra29in@yahoo.co.in

Introduction

In recent years the development of molecular sensors for recognizing both ionic and neutral species has been a subject of intense research interest in modern sensing arena because of their wide application in the fields of drug development, medicine, cancer detection, photosensitization, environmental monitoring and explosive detection etc.¹ Out of various metal ions aluminum being the most prevalent (8.3% by weight) metallic element and the third most abundant of all elements (after oxygen and silicon) in the earth's crust, is not only used in industrial fields for example water treatment, food additives, and medicines, production of light alloy but also it is profusely used in our daily life as electronic and electrical components of different implements, building materials, various packaging items etc.² However, the unregulated amounts of aluminum in human body may lead to the malfunction of central nervous system, Parkinson's disease, Alzheimer's disease and amyotrophic lateral sclerosis.³ Apart from this, the toxicity of aluminum endangers the aquatic life and influences agricultural production in acidic soils. The acidity of soil is due to the sorption of H^+ and Al^{3+} ions to soil surface, and further reaction of Al^{3+} with water releases extra H^+ ions. The high Al^{3+} content effects the growth of plants: (a) at the root tip, it interferes with the uptake of Ca^{2+} , the latter is an essential plant nutrient (b) results in the alteration of the physiological and biochemical processes of plant and (c) can restrict cell wall expansion leading to stunted roots.⁴⁻⁸ In spite of its many drawbacks, the use of Al cannot be circumvented in modern life and hence there is a good chance of Al^{3+} toxicity towards human health and the environment. Therefore detection of Al^{3+} is crucial in controlling its concentration levels in the biosphere and its direct impact on human health.

Likewise, bisulphite ion (HSO_3^-) among various anions has chemical and biological significance. Bisulfite (HSO_3^-) anions are widely used as essential preservatives for foods, beverages, and pharmaceutical products to prevent oxidation, browning, and microbial reactions during production and storage. In fact, addition of bisulfite to beer and wine has been customary for centuries in most countries. It is widely used for bisulfite treatment of DNA and as additive to the drug epinephrine.⁹ However, exposure to excess bisulphite can stimulate various health issues like asthmatic, allergic problems, reproductive and developmental toxicity.¹⁰ Thus, risk of uncontrolled release of this ion in ecosystem has attracted the chemists to formulate new reagents that allow flexible and in- expensive instrumentation for their analytical studies.

The development of a chemo-sensor, which is capable of recognizing both a metal ion and an anion simultaneously, is one of the most significant tasks because of its important potential applications in biological industry and environmental processes.¹¹ In addition, the detection of multiple targets with a single receptor would be more efficient and at the same time less expensive than a one-to-one analysis method, and therefore would attract more attention.¹² Among various approaches for the detection of both metal ions and anions, especially the fluorometric and colorimetric methods are more popular because of their high sensitivities, easy operation, rapid response rates and relatively low costs.

Herein, we report a simple, easy to prepare and cost effective chemo sensor (*N*¹*E,N*⁴*E*)-*N*¹,*N*⁴-bis(pyridine-4-ylmethylene)benzene-1,4-diamine (**L**) for simultaneous selective detection of Al³⁺ and HSO₃⁻ in aqueous media. The chemo-sensor **L** demonstrated the presence of the cation, Al³⁺ by both fluorescence enhancement and colorimetrically and that of anion HSO₃⁻ with an instant change of colour from yellow to colourless. The sensor was successfully applied in detection of Al³⁺ in bovine serum albumin. Moreover, **L** could be used as a practical, visible colorimetric test kit in an aqueous environment.

Experimental

General information

Fluorescence spectra were recorded on a Hitachi spectrophotometer. UV/Visible spectra were recorded on a Shimadzu UV 1800 spectrophotometer using a 10 mm path length quartz cuvette. ¹H NMR spectra were recorded on a Bruker Ultrashield 600 (for Al³⁺ titration) and 400 MHz spectrometer (for HSO₃⁻ titration). The NMR (¹H & ¹³C) spectra of ligand were obtained in DMSO-d₆ and NMR titrations were carried out dissolving **L** and metal salts in DMSO-d₆ and D₂O (9/1, v/v) respectively at room temperature and the chemical shifts are reported in δ values (ppm) relative to TMS. High resolution mass (HRMS) spectra were recorded on Waters mass spectrometer using mixed solvent HPLC methanol and triple distilled water. The measurements of pH were done using a digital pH meter (Merck). All the chemicals and metal salts were purchased from Merck. Manganese salt is sulphate while the rest of the metal salts used are nitrates and re-crystallized from water (Millipore) before use. Solutions of the receptor **L** (1 × 10⁻⁵ M) and metal salts (1 × 10⁻⁴ M) were prepared in CH₃OH–H₂O (2/1, v/v) and H₂O respectively.

Synthesis and characterisation of **L**

To a dehydrated methanolic solution of *p*-phenylenediamine (0.108 g, 1 mmol, in 50 mL methanol) pyridine-4-carboxaldehyde in methanol (0.214 g, 2 mmol, in 5 mL methanol) was added. The mixture was refluxed for 4h at 45^oC, maintaining dry condition. A yellow precipitate obtained was filtered and washed several times with *n*-hexane and then again recrystallized in methanol and dried in a vacuum to obtain the pure yellow solid. Yield: 82%. M.P- 205^oC. ¹H NMR: (DMSO-*d*₆, δ ppm, TMS): 8.77 (d, 4H); 8.75 (s, 2H); 7.87 (d, 4H) and 7.46 (s, 4H) (Fig. S1); ¹³C NMR: (DMSO-*d*₆, δ ppm, TMS): 160.4, 152.1, 150, 148.6, 142.9, 122.6, 114 (Fig. S2). FT-IR: (KBr, cm⁻¹): 1597.08 (C=N). ESI-MS: *m/z* [M + H⁺], 288.48 (100%) (Fig. S3). Anal. calcd for C₁₈H₁₄N₄: C, 75.50; H, 4.93; N, 19.57%. Found C,75.54; H,4.91; N,19.59%.

Fluorescence Titration

L (2.86 mg) was dissolved in 10 mL of mixed solvent CH₃OH–H₂O (2/1, v/v) to make a solution of 1 × 10⁻³ M and 30 μL of this solution were diluted with 2.97 mL of solvent mixture to make the final concentration of 10 μM, Al(NO₃)₃(37.5mg) was dissolved in triple distilled water (10 mL) and 1.5–90 μL of this Al³⁺ solution (10 mM) were transferred to each receptor solution (10 μM) to give 0.5–30 equiv. After mixing them for a few seconds, fluorescence spectra were obtained at room temperature.

UV-Vis titrations

For Al³⁺, **L** (2.86 mg, 0.01 mmol) was dissolved in afore-mentioned solvent mixture (10 mL) and 30 μL of it was diluted to 3 mL with the solvent mixture to make a final concentration of 10μM. Al(NO₃)₃ (37.5mg, 0.1 mmol) was dissolved in 10 mL of triple distilled water and 1.5–90 μL of the Al³⁺ ion solution (10 mM) were transferred to the solution of **L** (10 μM) prepared above. After mixing them for a few seconds, UV-Vis spectra were obtained at room temperature.

For HSO₃⁻, the concentration and volume of the solution of **L** was same as mentioned before. Sodium bisulphite (10.4 mg, 0.1 mmol) was dissolved in triple distilled water (10 mL) and 0.3–30 μL of the HSO₃⁻ solution (10 mM) were transferred to the solution of **L** (10 μM) prepared above. After mixing them for a few seconds, UV-Vis spectra were obtained at room temperature.

Job plot measurements

For Al^{3+} , **L** (2.86 mg, 0.01 mmol) was dissolved in methanol (10 mL). 100, 90, 80, 70, 60, 50, 40, 30, 20, 10 and 0 μL of the **L** solution were taken and transferred to vials. Each vial was diluted with 2.9 mL of mixed solvent. $\text{Al}(\text{NO}_3)_3$ (0.01 mmol) was dissolved in triple distilled water (10 mL). 0, 10, 20, 30, 40, 50, 60, 70, 80, 90 and 100 μL of the Al^{3+} solution were added to each diluted **L** solution. Each vial had a total volume of 3 mL. After shaking them for a minute, UV-Vis spectra were obtained at room temperature.

Competition with other metal ions or anions

For Al^{3+} , **L** (2.86 mg, 0.01 mmol) was dissolved in afore-mentioned solvent mixture (10 mL) and 30 μL of it was diluted to 3 mL with the solvent mixture to make a final concentration of 10 μM . $\text{Al}(\text{NO}_3)_3$ (37.5mg, 0.1 mmol) and $\text{M}(\text{NO}_3)_x$ (0.1 mmol) was dissolved in 10 mL of triple distilled water. 30 μL of each metal solution (10 mM) were taken and added to 3 mL of the solution of receptor **L** (10 μM) to give 10 equiv. of metal ions. Then, 30 μL of Al^{3+} solution (10 mM) were added to the mixed solution of each metal ion and **L** to make 10 equiv. After mixing them for a few seconds, fluorescence spectra were obtained at room temperature.

For HSO_3^- , **L** (2.86 mg, 0.01 mmol) was dissolved in methanol (10 mL) and 30 μL of this solution was diluted to 3 mL with the above-mentioned solvent mixture to make the final concentration of 10 μM . Sodium salts of F^- , Cl^- , Br^- , I^- , N_3^- , H_2PO_4^- , NO_3^- , OAc^- , HCO_3^- and HSO_3^- (0.1 mmol) were dissolved in 10 mL of triple distilled water and 30 μL of each solution (10 mM) were added to 3 mL of the solution of receptor **L** (10 μM) to give 10 equiv. of anion conc. Then, 30 μL of HSO_3^- solution (10 mM) were added to the mixed solution of each anion and **L** to make 10 equiv. After mixing them for a few seconds, absorbance spectra were obtained at room temperature.

pH effect test

A series of buffers with pH values ranging from 2 to 12 was prepared using 100 mM HEPES buffer. After the solution with a desired pH was achieved, receptor **L** (2.86 mg, 0.01 mmol) was dissolved in methanol (10 mL), and then 30 μL of this solution (1 mM) was diluted to 3 mL with above-mentioned buffers to make the final concentration of 10 μM . $\text{Al}(\text{NO}_3)_3 \cdot 9\text{H}_2\text{O}$ (37.5 mg, 0.1 mmol) was dissolved in HEPES buffer (10 mL, pH 7.00). 30 μL of the Al^{3+} solution (10 mM)

were transferred to each receptor solution (10 μM) prepared above. After mixing them for a few seconds, fluorescence spectra were obtained at room temperature.

^1H NMR titrations

For ^1H NMR titrations of receptor **L** eight NMR tubes of receptor **L** (2.86 mg, 0.01 mmol) dissolved in $\text{DMSO-}d_6$ (700 μL) were prepared and then three different concentrations (0, 0.01, 0.02, and 0.05 mmol) of aluminium nitrate dissolved in D_2O were added to each solution of receptor **L**. After shaking them for a minute, ^1H NMR spectra were obtained at room temperature.

For HSO_3^- five different concentrations (0, 0.005, 0.01, 0.02, 0.05 mmol) of Sodium bisulphite dissolved in D_2O were added to each solution of receptor **L**. After shaking them for a minute, ^1H NMR spectra were obtained at room temperature.

Colorimetric test kit

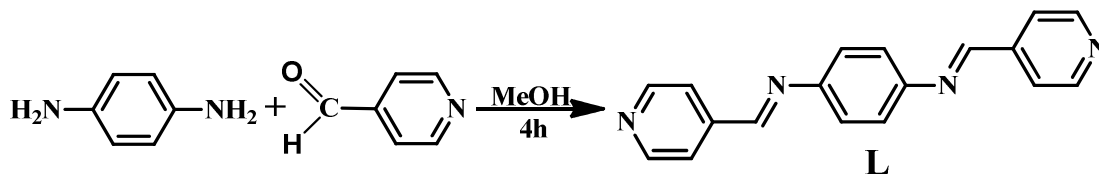
Receptor **L** (2.86 mg, 0.01 mmol) was dissolved in a mixture of $\text{CH}_3\text{OH-H}_2\text{O}$ (2/1, v/v, 10 ml) to get 1mM solution. Receptor **L**-test kits were prepared by immersing filter-papers into this receptor **L** solution (1 mM), and then dried in air. Sodium salts (F^- , Br^- , Cl^- , I^- , AcO^- , H_2PO_4^- , N_3^- , HSO_3^- , NO_3^- , HCO_3^- ; 0.001 mmol) were dissolved in (10 mL) to prepare 0.1 mM solution. The test kits prepared above were added into different anion solutions (1 mL), and then dried at room temperature.

Measurements of bisulfite in food samples

The food samples - red sugar, crystal sugar and granulated sugar were purchased from a supermarket and were used in the real sample analysis. Sugar sample solutions were prepared by dissolving 3 g of different sugar in deionized water and diluting to 10 mL. Aliquots of the food sample solution were added directly to the receptor **L** (10 μM) and after 5 min, the absorption intensity at 290 nm was recorded. Aliquots of the food samples were then spiked with different concentrations of NaHSO_3 (0.5 or 1 μM) that had been accurately prepared. The resulting samples were then treated with the receptor **L** (10 μM) for 5 min and the absorption intensity at 290 nm was recorded.

Results and discussion

Synthesis and structure of **L**

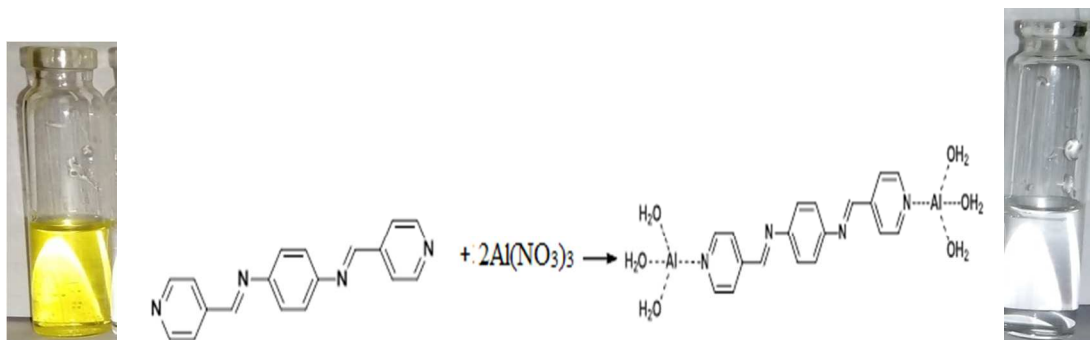


Scheme 1 Synthetic procedure of the receptor **L**

Bright yellow solid receptor **L** was obtained by the condensation reaction of p-phenylenediamine and pyridine-4-carboxaldehyde in methanol with 82% yield (scheme 1), and characterized by ^1H NMR and ^{13}C NMR, IR and ESI-mass spectrometry and elemental analysis. Jiang *et al*¹³ reported the X-ray single crystal structure of **L** in 2007. **L** was used as bridging ligand for the construction of supramolecular complexes.^{14,15} E. Schab-Balcerza¹⁶ studied structural, thermal, optical, and electrochemical properties of **L**.

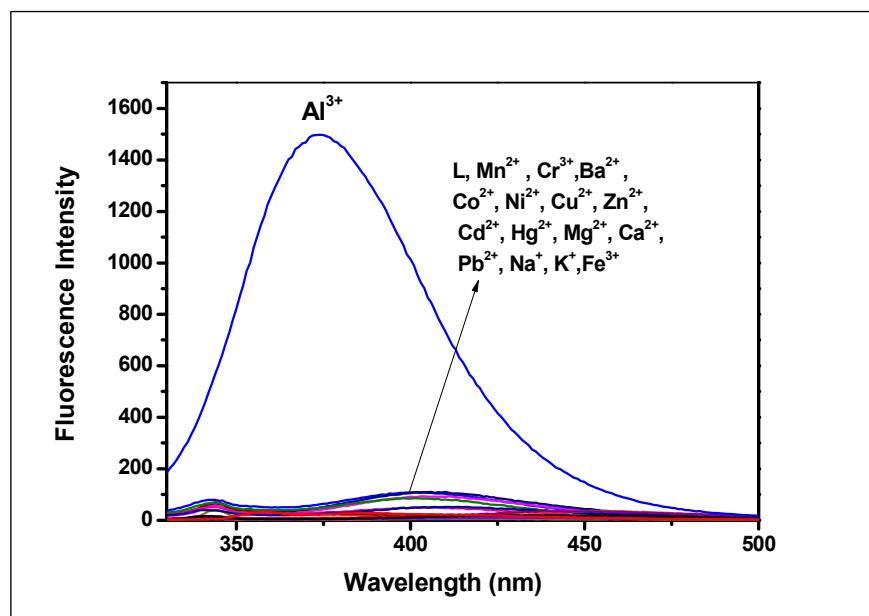
Fluorescence and absorption studies of **L** towards different metal cations

The fluorescence behaviours of receptor **L** towards various metal ions (Na^+ , K^+ , Mg^{2+} , Ba^{2+} , Mn^{2+} , Fe^{3+} , Co^{2+} , Ni^{2+} , Cu^{2+} , Zn^{2+} , Cd^{2+} , Ca^{2+} , Cr^{3+} , Hg^{2+} , Pb^{2+} and Al^{3+}) were investigated in methanol-water (2/1, v/v) as shown in Fig. 1a. Upon excitation at 310 nm at room temperature **L** exhibits little emission with a low fluorescence quantum yield ($\Phi = 0.0169$) along with other metal ions except for Al^{3+} ($\Phi = 0.763$). This low fluorescence intensity of **L** can be ascribed to the photoinduced electron transfer (PET) process caused by the electron transmission from the two terminal pyridyl nitrogen atoms to the large π conjugation system including two $>\text{C}=\text{N}-$ groups and three aromatic rings. On addition of Al^{3+} , **L** is coordinated to metal by supplying its lone pair electrons on pyridyl nitrogen atoms and thereby hinders the PET process resulting a significant fluorescence enhancement of **L**- Al^{3+} complex accompanied by a prominent blue shift of 28 nm. In conjunction, stable chelate complexation of Al^{3+} with **L** possibly induces rigidity in the resulting complex thereby generating efficient chelation enhanced fluorescence (CHEF)¹⁷ (Scheme 2).



Scheme 2 Sensing mechanism of **L**- Al^{3+} complex

The fluorescence enhancement efficiency observed was 106-fold greater than the control in absence of Al^{3+} (Fig. 1b). This unique selectivity of receptor **L** for Al^{3+} could be interpreted in terms of the smaller ionic radius and higher charge density of the Al^{3+} . In this connection absorption study also reflects the preferential selectivity of **L** towards Al^{3+} over the aforementioned metal ions (Fig. S4).



(a)

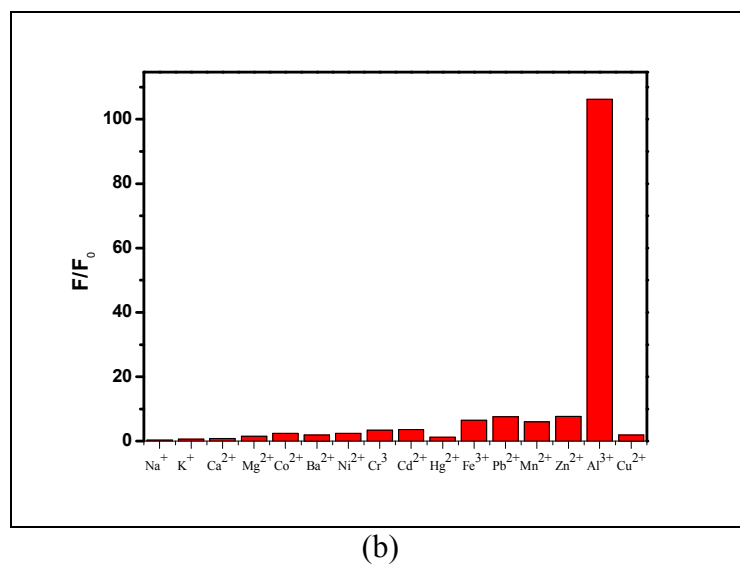


Fig. 1 (a) Fluorescence spectra of **L** (10 μM) before and after addition of various metal ions (100 μM) of Mn^{2+} , Fe^{3+} , Co^{2+} , Ni^{2+} , Cu^{2+} , Zn^{2+} , Cd^{2+} , Hg^{2+} , Na^+ , K^+ , Mg^{2+} , Ca^{2+} , Al^{3+} , Pb^{2+} , Cr^{3+} and Ba^{2+} in methanol-water (2:1, v/v) (b) Bar graph shows the relative emission intensity of **L** at 373 nm upon treatment with various metal ions.

A quantitative investigation of the binding affinity of **L** with Al^{3+} was performed by a fluorescence titration (Fig. 2). It revealed that the emission intensity at 373 nm monotonically increased upon gradual addition of Al^{3+} up to 30 equiv. The inset plot of Fig. 2 which elaborates the titration data in narrow range shows that the F/F_0 curve becomes a plateau at the $[\text{Al}^{3+}]/[\text{L}]$ ratio over 2. This is well corroborated by the UV-visible spectrometric titration of **L** with Al^{3+} solution (Fig. 3). It illustrates the variation of UV spectrum of **L** along with the increasing amounts of Al^{3+} from 0 to 10 equiv. Three absorbance bands were observed on the spectrum of **L** at 240 nm, 287 nm, 368 nm. Among them two strong bands at 240 nm and 368 nm were assigned to the phenyl π - π^* and n - π^* electron transition respectively. As shown in Fig. 3, with increasing conc. of Al^{3+} , the intensity of absorption bands at 240 nm and 287 nm increases whereas the absorption band at 368 nm decreases causing an isosbestic point at 314 nm which indicates that only one product was generated from **L** upon binding to Al^{3+} . The Job plot analysis indicated 1:2 stoichiometric complexation of receptor **L** with Al^{3+} (Fig. S5). In addition, the formation of a 1:2 complex between **L** and Al^{3+} was further confirmed by the appearance of a peak at m/z 442, assignable to $[\text{L} + 2 \text{Al}^{3+} + 6 \text{H}_2\text{O} - 6 \text{H}^+]$ in the ESI/MS (Fig. S6). From the fluorescence titration

profiles, the association constant for $L-Al^{3+}$ in MeOH-H₂O (2:1, v/v) was determined as $1.26 \times 10^5 M^{-1}$ by a Hill plot (Fig. S7). By using the above-mentioned titration results, the detection

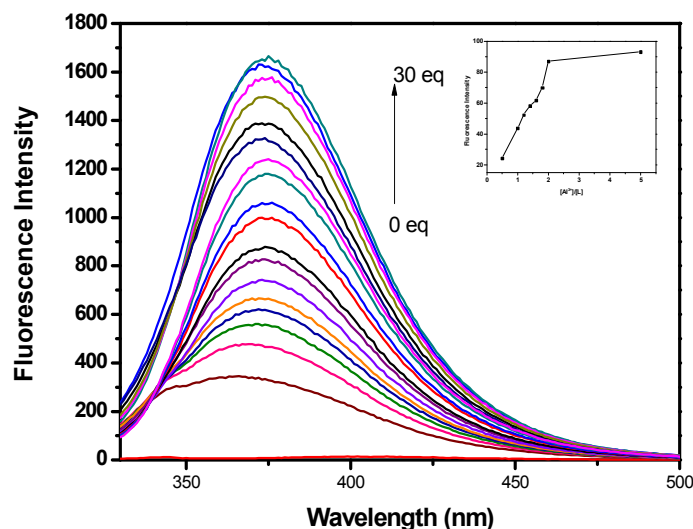


Fig. 2 Fluorescence spectra of **L** (10 μM, $\lambda_{ex} = 310$ nm) after addition of increasing amounts of Al^{3+} (upto 30 equiv.) in MeOH-H₂O (2:1, v/v) at room temperature. Inset: intensity at 373 nm vs the number of equiv. of Al^{3+} added.

limit for the $L-Al^{3+}$ complex was determined to be 0.903 μM on the basis of $3\sigma/K$. Importantly, the detection limit of **L** is much lower than the WHO limit¹⁸ and suggests that **L** could be an effective sensor for the detection of aluminum in drinking water.

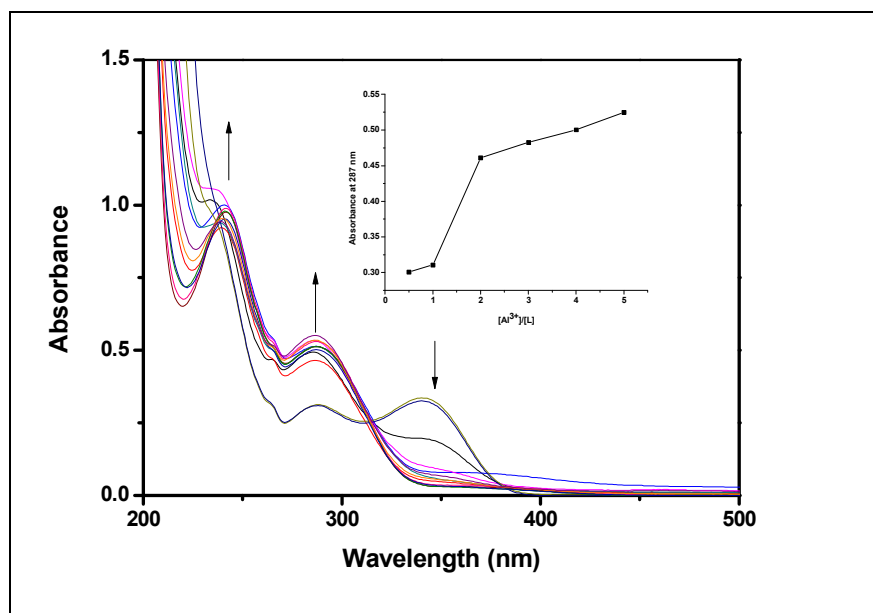


Fig 3. Absorption spectra of **L** changes after addition of Al^{3+} upto 10 equiv. in MeOH- H_2O (2:1, v/v) at room temperature. Inset: Absorption at 368 nm vs the number of equiv. of Al^{3+} added.

To further check the practical applicability of receptor **L** as an Al^{3+} -selective fluorescence receptor, a competitive experiment was carried out with 10 equiv. of Al^{3+} in presence of other metal ions in an aqueous solution (Fig. 4). It was found that most of the metal ions did not interfere with the detection of Al^{3+} by **L**. However, Fe^{3+} and Cr^{3+} quenched about 36 and 45% of the fluorescence obtained with Al^{3+} alone respectively. Nevertheless, **L** still had sufficient “turn-on” ratios for the detection of Al^{3+} in the presence of Fe^{3+} and Cr^{3+} . These results indicate that **L** could be a good sensor for Al^{3+} over competing metal ions.

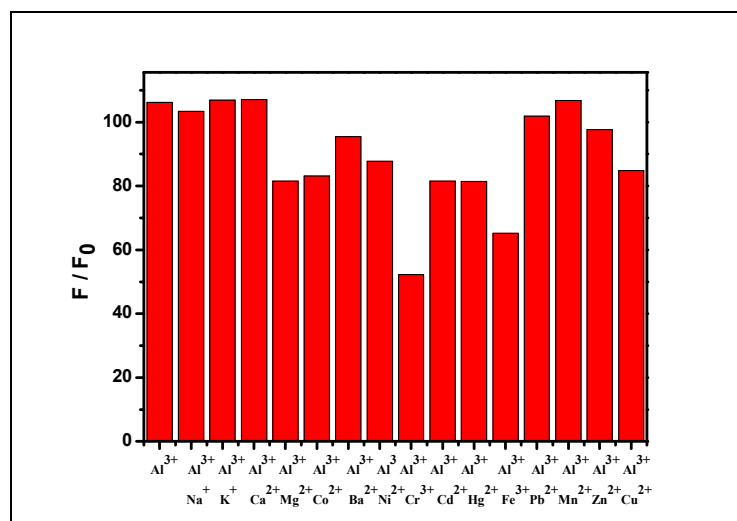


Fig. 4 Relative fluorescence of **L** and its complexation with Al^{3+} in the presence of various metal ions - $\text{L} + \text{Al}^{3+}$, $\text{L} + \text{Al}^{3+} + \text{Na}^+$, $\text{L} + \text{Al}^{3+} + \text{K}^+$ etc. (left to right) $\lambda_{\text{ex}} = 310 \text{ nm}$.

To check the pH effect, the fluorescence of receptor **L** under different pH conditions was examined using 100 mM HEPES buffer (Fig. 5). For L-Al^{3+} complex, the fluorescence intensity does not differ from ligand at pH 2-3 and reaches maxima at pH 6 in 2 to 12 pH range with slight decrease in intensity at 11. This fluorescence behaviour of both, **L** and L-Al^{3+} permits its application under physiological conditions for wide pH range of 4-11 without hampering the detection results. For practical applications, the real-time determination was also important. The time evolution of receptor **L** in the presence of 10.0 equiv. of Al^{3+} in MeOH-H₂O was investigated as shown in Fig. S8(a), the recognition interaction gets almost completed just after the addition of Al^{3+} and the fluorescence intensity remain almost same up to 10 min. This ensures the receptor **L** to be a sensitive sensor which can be applied in environmental analysis.

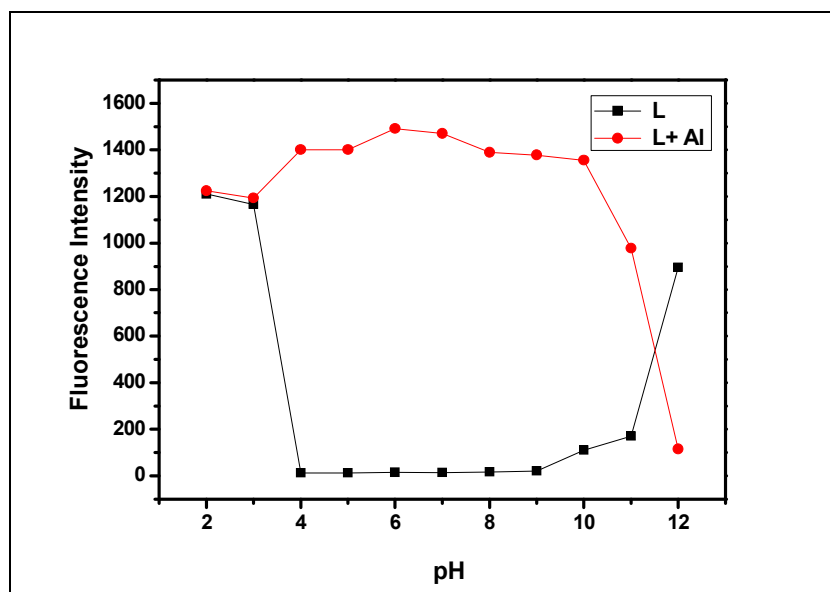
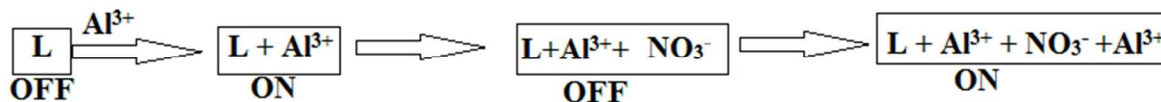


Fig. 5 Fluorescence intensity of L-Al^{3+} (**L**, 10 μM) after addition of 10 equiv. of Al^{3+} at various ranges of pH in MeOH-H₂O (2:1, v/v) at room temperature. Inset: intensity at 373 nm.

Reversibility is a prerequisite in developing novel chemosensors for practical applications. The reversibility of **L** towards the Al^{3+} ion was checked using different anions and disodium salt of ethylenediamine tetraacetate (Na_2EDTA). The fluorescence intensity of the L-Al^{3+} complex was

found to be quenched upon the addition of more than ten equiv. of NaNO_3 . This fluorescence quenched solution regained its fluorescence after the addition of $\text{Al}_2(\text{SO}_4)_3$ (Scheme 3).



Scheme 3 Schematic presentation for reversibility of sensor **L**

In above experiment, on addition of NaNO_3 in much higher concentration (>10 equiv.) to the **L**- Al^{3+} complex in aqueous medium the nitrate ion substitutes **L** and binds with Al^{3+} thereby quenching the fluorescence intensity of the complex. But such phenomenon does not occur in competitive experiment (Fig. 4). In this case aqueous solution of $\text{Al}(\text{NO}_3)_3$ (10 equiv.) was added to the mixed solution of **L** and NaNO_3 . As Na^+ does not form complex with the ligand, it cannot interfere in Al^{3+} -**L** complexation process. Consequently the fluorescence enhancement occurred as is observed in absence of NaNO_3 . In reversible experiment fluorescence quenched solution containing free ligand regained its fluorescence on addition of $\text{Al}_2(\text{SO}_4)_3$ because the added Al^{3+} got complexed with the free ligand. In Fig. 6 the reversible fluorescence switching cycles based on the intensity at 373 nm has been shown. Interestingly the addition of Na_2EDTA has no effect on the fluorescence intensity of the **L**- Al^{3+} complex. The fluorescence spectrum of **L**- Al^{3+} complex after addition of Na_2EDTA has been provided in ESI section (Fig S9)

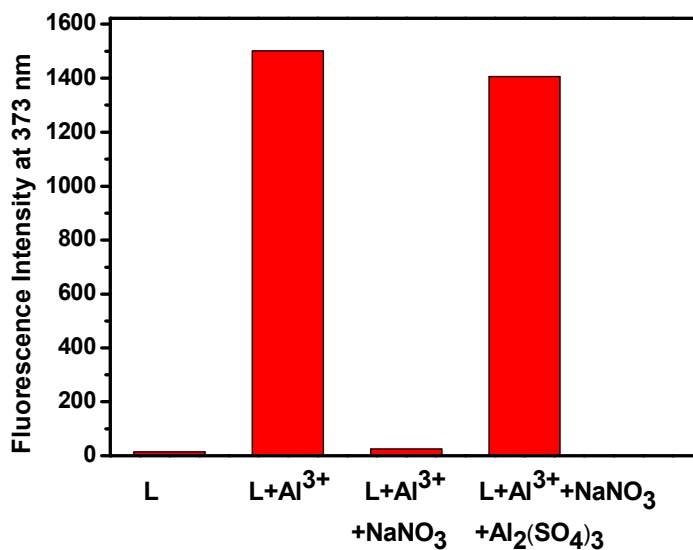


Fig. 6 Reversible fluorescence switching cycle

To further explore the complexation behaviour of receptor **L** with Al^{3+} , ^1H NMR titration experiments were carried out in mixed solvent $\text{DMSO-d}^6\text{-D}_2\text{O}$. The spectral differences are depicted in Fig. 7. In the free ligand **L**, the protons resonate at 8.77, 8.75, 7.87 and 7.46 ppm, out of which protons at 8.75 ppm may be assigned as imine protons. The imine protons as well as the aromatic protons of **L** shifted towards upfield, upon the addition of Al^{3+} upto 2 equiv. No significant shift of these peaks is observed in increasing the concentration of Al^{3+} ensuring the formation of 1:2 complex between the **L** and Al^{3+} .

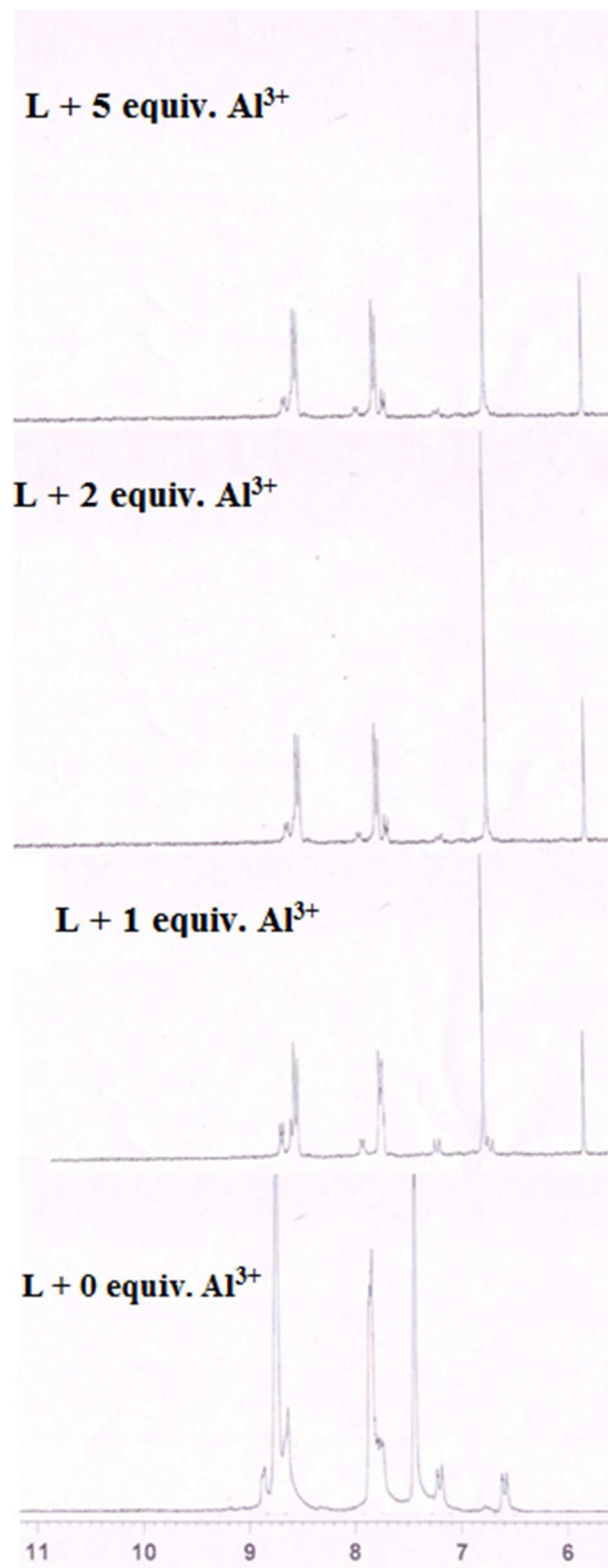


Fig. 7 ^1H NMR Titration of **L** with Al^{3+} in d_6 -DMSO- D_2O (9/1, v/v)

To understand the aggregation property of **L** and $[Al_2L]$, and its effect on their chemosensing property, scanning electron microscope (SEM) imaging was carried out. **L** and $[Al_2L]$ possess charge transfer, π - π stacking, and van der Waals force of attraction which cause the compounds to form a sheet-like 2D nanostructure and agglomerate material respectively (Fig. S10a and b). The aggregation mechanism might be due to the strong complexation of Al^{3+} -ion with the ligand **L**.

Application of chemosensor **L** in biological sample

The results of the pH dependence and time dependence experiment prompted us to test whether the determination of Al^{3+} in biological sample can be monitored by fluorimetry. The sensor **L** was successfully utilised in the determination of Al^{3+} in aqueous solution of bovine serum albumin (BSA) protein. Fig. 8 shows the fluorescence intensity enhancement for **L** in BSA medium. The inset is the plot of fluorescence intensity of **L** as a function of Al^{3+} concentration. An enhancement in fluorescence intensity of about 71 times has been observed.

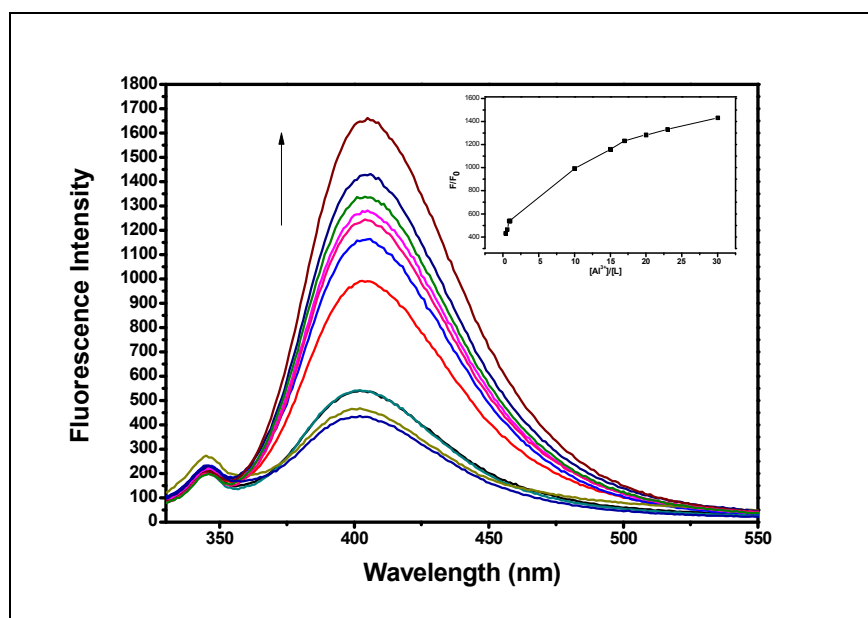


Fig. 8 In aqueous bovine serum albumin medium-fluorescence spectra of **L**. Inset: plot of fluorescence intensity versus Al^{3+} concentration.

Colorimetric and spectral response of **L** towards HSO_3^-

The colorimetric selective sensing abilities of receptor **L** with various anions in a mixture of methanol-H₂O (2 : 1, v/v) were also investigated by UV-Vis absorption spectrometry (Fig. 9). Only the addition of HSO₃⁻ induced distinct spectral changes while other anions (F⁻, AcO⁻, Cl⁻, Br⁻, I⁻, H₂PO₄⁻, HCO₃⁻, N₃⁻, NO₃⁻) did not induce any spectral changes. Consistent with the change in UV-Vis spectra, the solution of **L** resulted in an immediate colour change from yellow to colourless with bisulphite ion (Fig. 10), indicating that receptor **L** can serve as a ‘naked-eye’ bisulphite indicator in aqueous solution.

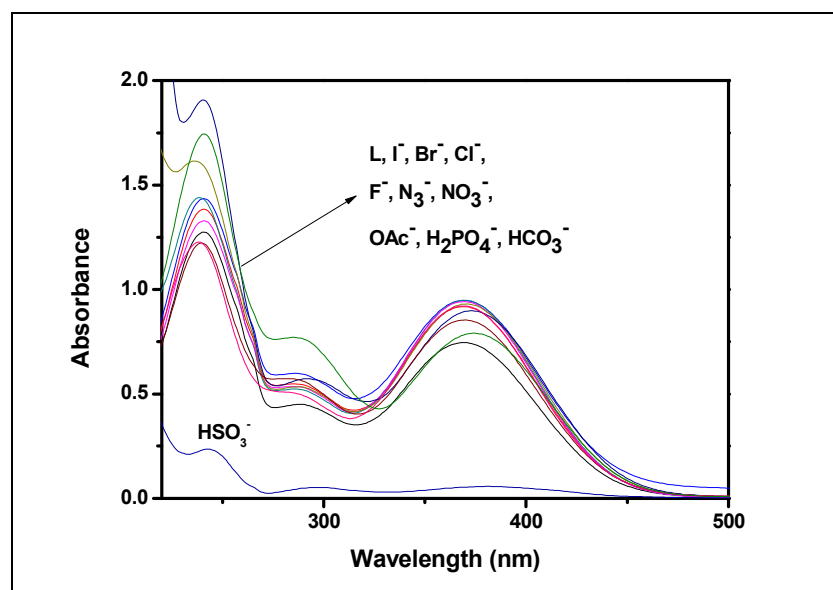


Fig. 9 Absorption spectral changes of **L** (10 μ M) in the presence of 10 equiv. of different anions in MeOH-H₂O (2:1, v/v) at room temperature.

The binding properties of **L** with HSO₃⁻ were further studied by UV-Visible titration experiment. As shown in Fig. 11, an increase in the absorption bands at 242 nm and 290 nm occurred with simultaneous decrease in absorption band at around 380 nm upon gradual addition of HSO₃⁻ developing an isosbestic points at 335 nm. A prominent red shift of about 12 nm was observed at 368 nm. This bathochromic shift of the absorption bands led us to propose that the π conjugate system of **L** underwent intramolecular charge transfer (ICT) from the donor to the acceptor upon excitation by light. Binding of HSO₃⁻ with **L** affected the efficiency of ICT and reduced the electron-donating ability of imino nitrogen atoms leading to the decrease in intensity at 368 nm. To identify the ICT property of **L**, we have checked the change of its absorption spectra in several solvents such as dimethylsulfoxide, methanol, ethanol and acetonitrile because it has been

reported that the solvent dipole can relax the ICT excited by polar solvents.¹⁹ As shown in Fig. S11 and summarized in Table 1, the absorption spectra of **L** featured a marginal red-shift of absorption

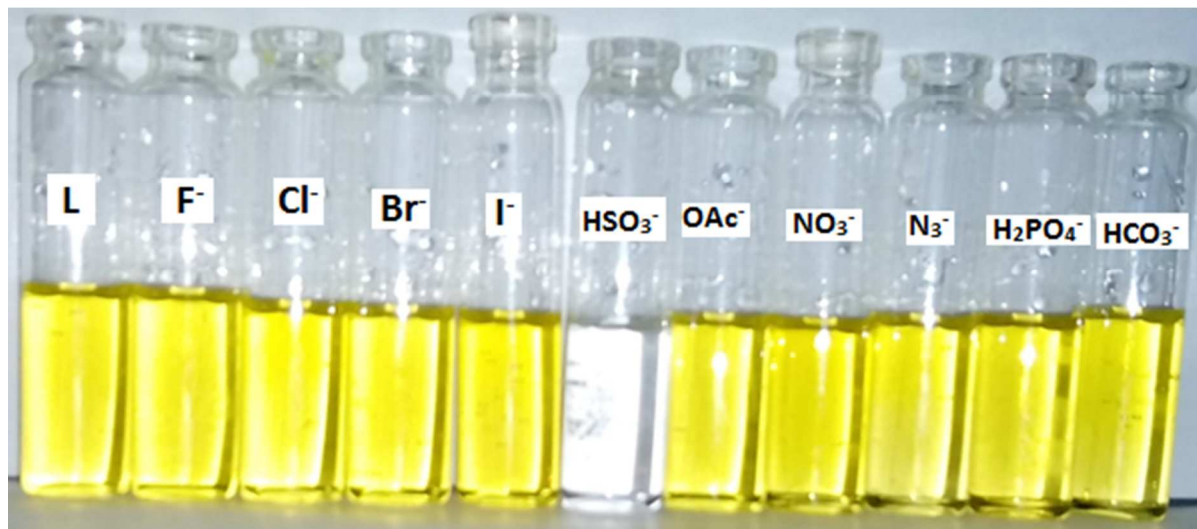


Fig. 10 The colour changes of **L** (10 μM) upon addition of various anions (10 equiv.) in MeOH-H₂O (2:1, v/v) at room temperature.

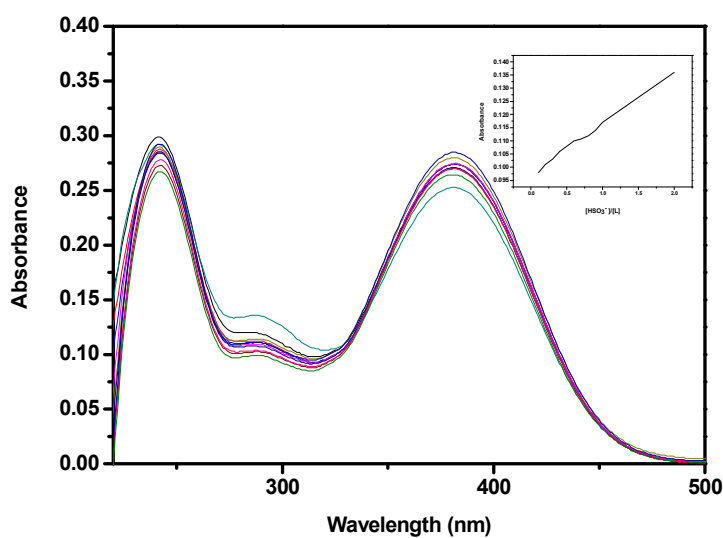


Fig. 11 Absorption spectra of **L** (10 μM) changes after addition of increasing amount of HSO_3^- upto 2 equiv. Inset: Absorption at 368 nm vs. the number of equiv. of HSO_3^- added.

maxima ($\Delta\lambda_{\text{abs}} = 13 \text{ nm}$), indicating an apparent solvent dependence of the absorption band. Therefore, this solvatochromic behaviour demonstrates the occurrence of the ICT transition in receptor **L**.^{11,19}

In order to get insight into the mechanism of optical detection of the HSO_3^- , the pH of the bisulphite solution ($10 \mu\text{M}$) was checked at room temperature. The observed pH ambience (6.74) is not sufficient to hydrolyse **L** in presence of HSO_3^- ion and thus confirmed the fact that the colour and spectral change occurred in sensing HSO_3^- ion was solely due to H-bonding between imino- N atom and HSO_3^- ion not due to hydrolysis. From the above mentioned UV titration profile the binding constant was determined to be 1.94×10^3 with a good linearity (0.9936) between absorption intensity and the conc. of HSO_3^- ($10 \mu\text{M}$ - $200 \mu\text{M}$) as shown in inset of Fig. 8.

Table 1 Absorption properties of **L** in various solvents

Solvent	λ_{abs} [nm] (log ϵ)
Ethanol	368 (6.92)
Methanol	373 (6.95)
Acetonitrile	378 (6.87)
DMSO	381 (7.09)

The preferential selectivity of **L** as a colorimetric chemosensor for the detection of HSO_3^- was studied in the presence of various competing anions. For competition tests, receptor **L** was treated with 10 equiv. of HSO_3^- in the presence of 10 equiv. of other anions. No interference was observed in the detection of HSO_3^- in the presence of other anions (Fig. 12). This result suggests that **L** could be an excellent sensor for selectively detecting HSO_3^- in the presence of the competing anions. To get more details on the spectral changes of probe **L** towards HSO_3^- , scanning kinetics were then performed. For HSO_3^- absorption intensity decreased suddenly within few seconds and remained almost constant up to 10 min on addition of 2 equiv. of HSO_3^- (Fig. S8b).



Fig. 12 The colour changes of **L** and its complexation with HSO_3^- in the presence of various anions in MeOH-H₂O (2:1, v/v) at room temperature. Conditions: **L**, 10 μM ; HSO_3^- , 10 equiv.; other anions, 10 equiv.

To elucidate the binding interaction of receptor **L** with HSO_3^- , ^1H NMR titration experiments were carried out in mixed solvent DMSO-*d*₆-D₂O. Upon addition of 2 equiv. of HSO_3^- to the receptor **L**, the ^1H NMR signal for imine proton disappeared, which illustrates the H-bond formation between bisulphite hydrogen and imino-nitrogen atom of **L** in 2:1 molar ratio (Fig. 13).

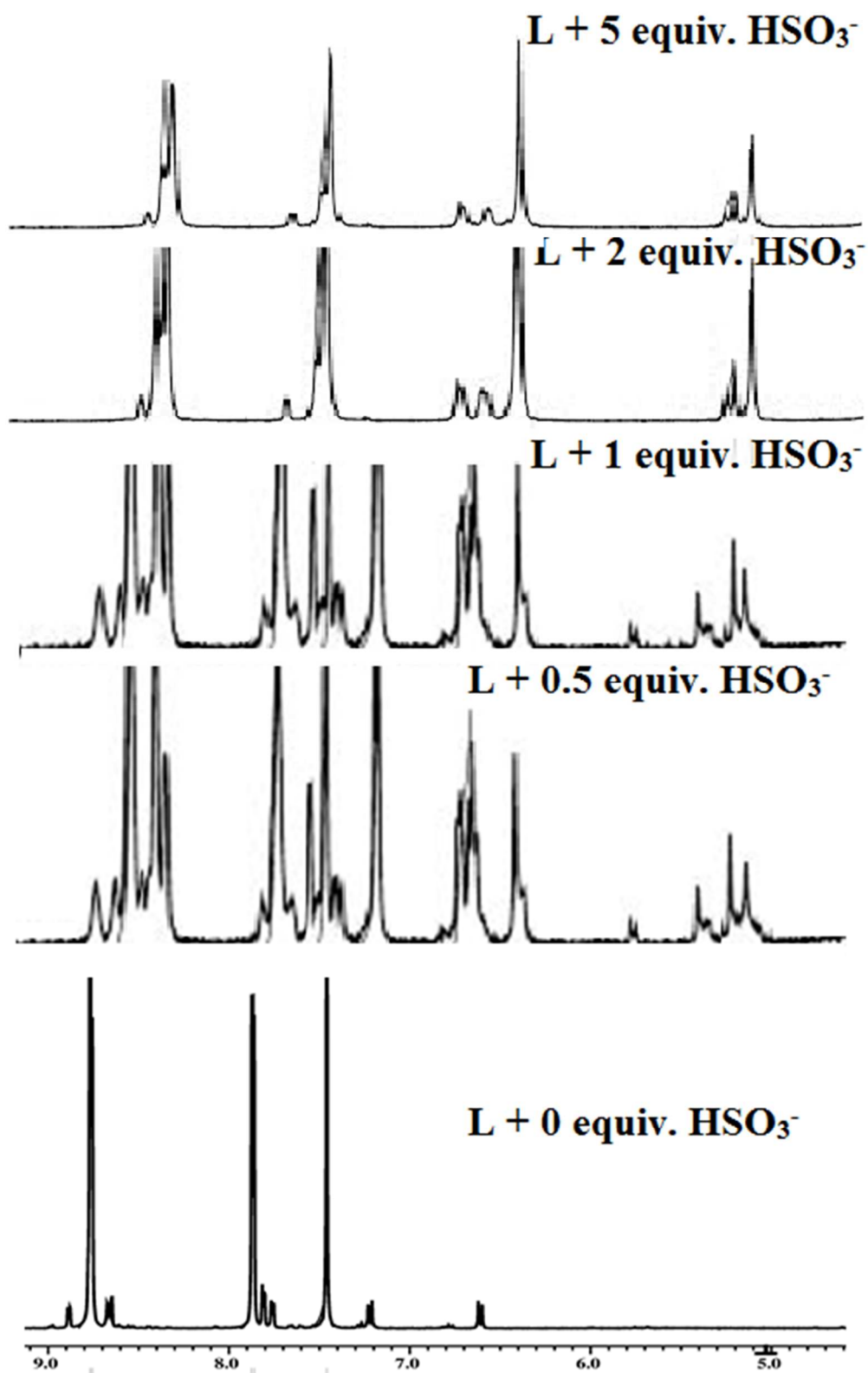


Fig. 13 ^1H NMR Titration of **L** with HSO_3^- in d_6 -DMSO- D_2O (9/1, v/v)

To check the practical application, the test kits were utilized to sense HSO_3^- among different anions. As shown in Fig. 14, when the test kits coated with **L** were added to different anion solutions, the obvious color change was observed only with HSO_3^- in methanol- H_2O solution (2 : 1, v/v). Therefore, the test kits coated with the receptor **L** solution would be convenient for detecting HSO_3^- . These results showed that receptor **L** could be a valuable practical sensor for environmental analyses of HSO_3^- .

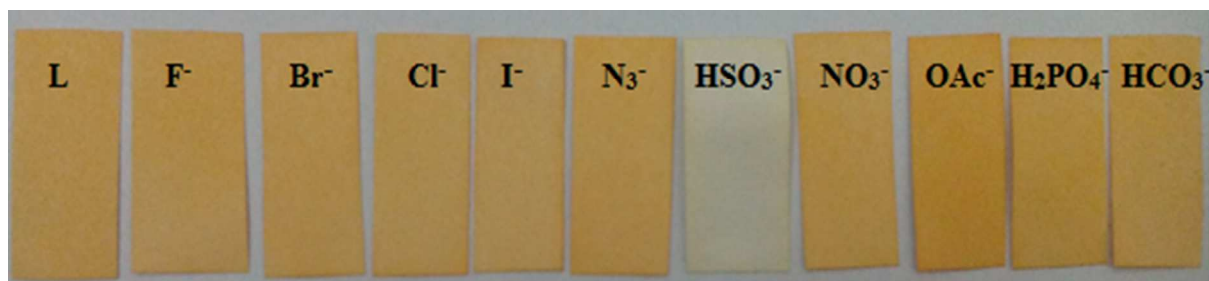


Fig. 14 Photographs of the test kits with **L** (0.5 mM) for detecting the bisulfite ion in neutral aqueous solution with other anions.

Measurements of bisulfite in food samples

We have investigated the potential of the receptor **L** to determine bisulfite in food samples. The red sugar, crystal sugar and granulated sugar were dissolved and diluted in water as the real food sample for analysis. As shown in Table 2, we can realize that the receptor **L** is able to determine the concentration of HSO_3^- in these real food samples with good recovery ranges from 98.5% to 101.91%, indicating that the bisulfite level in these food samples can be accurately measured by the receptor **L**.

Table 2 Determination of bisulphite in food samples

Sample	HSO_3^- level (μM)	Added (μM)	Found (μM)	Recovery(%)
Red Sugar	4.70	0.50	5.23	100.57
		1.00	5.75	100.8
Crystal Sugar	1.61	0.50	2.14	101.42
		1.00	2.66	101.91
Granulated Sugar	2.35	0.50	2.81	98.59
		1.00	3.30	98.50

Conclusion

In summary, we have successfully designed and synthesized a simple, fluorescent-colorimetric chemosensor **L**, capable of recognizing both cation and anion in aqueous solution. **L** exhibited an excellent selectivity and sensitivity towards Al^{3+} by both fluorescent intensity enhancement and colorimetrically and can sense HSO_3^- by inducing a rapid colour change from yellow to colourless. The detection limit of **L** for Al^{3+} ($0.903\mu\text{M}$) was much lower than that mentioned in guidelines of the WHO ($7.41\mu\text{M}$). Moreover, **L** could operate in a wide range of pH and can be successfully applied to biological samples for detecting Al^{3+} and for measurements of bisulfite in food samples. Although there are several reports of chemosensors based on rhodamine, coumarin, calixarene, pyrene, BODIPY, 8-hydroxyquinoline, anthraquinone, BINOL and other Schiff base molecules,²⁰ most of them suffers from some serious disadvantages such as poor water-solubility, laborious synthetic processes and interference from other coexisting metal ions, low detection limit and slow detection in practice etc. In addition, they are generally expensive and not suitable in constructing device. On the basis of these results, we believe that our receptor **L** will offer an important guidance to the development of single receptor for recognizing cation and anion both in vivo and in vitro.

Acknowledgement

G.K.P would like to thank the Department of Science and Technology and Department of Biotechnology, Government of India, New Delhi for financial support.

References:

- (a) M. Kumar, J.N. Babu and V. Bhalla, *Talanta.*, 2010, **81**, 9; (b) C. Gou, S. -H. Qin, H. -Q. Wu, Y. Wang, J. Luo and X. -Y. Liu, *Inorg. Chem. Commun.*, 2011, **14**, 1622; (c) Q. Lin, Y. -P. Fu, P. Chen, T. -B. Wei and Y. -M. Zhang, *Dyes Pigments.*, 2013, **96**, 1; (d) C. R. Wang and Q. B. Lu, *J. Am. Chem. Soc.*, 2010, **132**, 14710; (e) Y.-J. Kim, H. Kwak, S.J. Lee and C. Kim, *Tetrahedron*. 2006, **62**, 9635; (f) J.M. Berg and Y. Shi, *Science.*, 1996, **271**, 1081; (g) B. Valeur and I. Leray, *Coord. Chem. Rev.*, 2000, **205**, 3; (h) J.B. Pawley, *Handbook of Biological Confocal Microscopy*, Plenum, New York, 1995; (i) J.W. Lichtman and J.A. Conchello, *Fluorescence microscopy*, *Nat. Methods*, 2005, **2**, 910; (j) J. Wu, W. Liu, J. Ge, H. Zhang and

- P. Wang, *Chem. Soc. Rev.*, 2011, **40**, 3483; (k) S. Shanmugaraju and P. S. Mukherjee, *Chem. Chem. Eur. J.*, 2015, **21**, 6656; (l) A. Chowdhury and P.S. Mukherjee, *J. Org. Chem.*, 2015, **80**, 4064; (m) L. Zhao, S. Qu, C. He, R. Zhang and C. Duan, *Chem. Commun.*, 2011, **47**, 9387.
2. (a) D. R. Crapper, S. S. Krishnan and A. J. Dalton, *Science*. 1973, **180**, 511; (b) D. P. Perl and A. R. Brody, *Science*. 1980, **208**, 297; (c) E. House, J. Collingwood, A. Khan, O. Korchazkina, G. Berthon and C. J. Exley, *J. Alzheimers Dis.* 2004, **6**, 291; (d) J. Burgess, *Chem. Soc. Rev.* 1996, **25**, 85–92; (e) J. Barceló, C. Poschenrieder, *Environ. Exp. Bot.* 2002, **48**, 75–92; (f) S. Goswami, S. Paul and A. Manna, *RSC Adv.* 2013, **3**, 10639–10643; (g) A. Sahana, A. Banerjee, S. Lohar, A. Banik, S. K. Mukhopadhyay, D. A. Safin, M. G. Babashkina, M. Bolte, Y. Garcia and D. Das, *Dalton Trans.* 2013, **42**, 13311–13314.
3. (a) E. Altschuler, *Med. Hypotheses.*, 1999, **53**, 22–23; (b) B. Wang, W. Xing, Y. Zhao and X. Deng, *Environ. Toxicol. Pharmacol.*, 2010, **29**, 308–313; (c) J.R. Walton, *Neuro. Toxicol.* 2006, **27**, 385–394; (d) S.M.N.R. Narayanaswamy, *Analytical and Bioanalytical Chemistry*, 2006, **386**, 1235–1244; (e) J. S. Perlmutter, L. W. Tempel, K. J. Black, D. Parkinson and R. D. Todd, *Neurology*, 1997, **49**, 1432; (f) Y. W. Wang, M. X. Yu, Y. H. Yu, Z. P. Bai, Z. Shen, F. Y. Li and X. Z. You, *Tetrahedron Lett.*, 2009, **50**, 6169; (g) S. H. Kim, H. S. Cho, J. Kim, S. J. Lee, D. T. Quang and J. S. Kim, *Org. Lett.*, 2010, **12**, 560.
4. (a) H.E. Witters, *Environ. Toxicol. Chem.*, 1996, **15**, 986–996; (b) J.L. Yang, *Ann. Bot.*, 2006, **97**, 579–584; (c) L.V. Kochian and O.A. Hoekenga, *Annu. Rev. Plant Biol.*, 2004, **55**, 459–493; (d) E. Delhaize and P.R. Ryan, *Plant Physiol.* 1995, **107**, 315–321; (e) D.L. Godbold, E. Fritz and A. Huttermann, *Proc. Natl. Acad. Sci. U.S.A.*, 1988, **8**, 3888–3892; (f) R. W. Gensemer and R. C. Playle, *Crit. Rev. Environ. Sci. Technol.* 1999, **29**, 315; (g) Budimir, *Acta Pharm.*, 2011, **61**, 1; (h) P. Nayak, *Environ. Res.*, 2002, **89**, 101; (i) P. Zatta, *Coord. Chem. Rev.*, 2002, **228**, 271.
5. (a) C. Meriño-Gergichevich, M. Alberdi, A.G. Ivanov and M. Reyes-Díaz, *J. Soil. Sci. Plant Nutr.*, 2010, **10**, 217–243; (b) M.L. Mora, M.A. Alfaro, S.C. Jarvis, R. Demanet, P. Cartes, *Soil Use Manage*, 2006, **22**, 95–101; (c) Z. Rengel and W.H. Zhang, *New Phytol.*, 2003, **159**, 295–314.

6. (a) X. Jiang, B. Wang, Z. Yang, Y. Liu, T. Li and Z. Liu, *Inorg. Chem. Commun.*, 2011, **14**, 1224–1227; (b) S. Polizzi, E. Pira, M. Ferrara, M. Bugiani, A. Papaleo, R. Albera and S. Palmi, *NeuroToxicology*, 2002, **23**, 761–774.
7. (a) J. L. Yang, L. Zhang, Y. Y. Li, J. F. You, P. Wu and S. J. Zheng, *Ann. Bot.*, 2006, **97**, 579–584; (b) L. V. Kochian, O. A. Hoekenga and M. A. Piñeros, *Annu. Rev. Plant Biol.*, 2004, **55**, 459–493 (c) T. Han, X. Feng, B. Tong, J. Shi, L. Chen, J. Zhi and Y. Dong, *Chem. Commun.*, 2012, **48**, 416–418; (d) N. E. W. Alstad, B. M. Kjelsberg, L. A. Vøllestad, E. Lydersen and A. B. S. Poléo, *Environ. Pollut.*, 2005, **133**, 333–342.
8. (a) A. B. S. Poléo, K. Østbye, S. A. Øxnevad, R. A. Andersen, E. Heibo and L. A. øllestad, *Environ. Pollut.*, 1997, **96**, 129–139; (b) S. Sen, T. Mukherjee, B. Chattopadhyay, A. Moirangthem, A. Basu, J. Marek and P. Chattopadhyay, *Analyst.*, 2012, **137**, 3975–3981; (c) C. Chen, D. Liao, C. Wan and A. Wu, *Analyst.* 2013, **138**, 2527–2530.
9. (a) R.F. McFeeters, *J. Food Protect.*, 1998, **61**, 885.; (b) T. Fazio and C.R. Warner, *Food Addit. Contam.* 1990, **7**, 433–454; (c) S.L. Taylor, N.A. Higley and R.K. Bush, *Adv. Food Res.* 1986, **30**, 1–76; (d) H. Vally, N.L. Misso and V. Madan, *Clin. Exp. Allergy.* 2009, **39**, 1643–1651.
10. (a) L.G. Decnop-Weever and J.C. Kraak, *Anal. Chim. Acta*, 1997, **337**, 125–131; (b) X.F. Yang, X.Q. Guo and Y.B. Zhao, *Anal. Chim. Acta*, (2002) **456**, 121–128; (c) I. Sarudi and J. Kelemen, *Talanta*, 1998, **45**, 1281–1284; (d) S.K. Verma, M.K. Deb, *J. Agric. Food. Chem.*, 2007, **55**, 8319–8324.
11. (a) H. Y. Li, R. A. Lalancette and F. Jäkle, *Chem. Commun.* 2011, **47**, 9378–9380; (b) E. Tomat and S. J. Lippard, *Inorg. Chem.* 2010, **49**, 9113–9115; (c) G. V. Zyryanov, M. A. Palacios and P. Anzenbacher Jr., *Angew. Chem., Int. Ed.* 2007, **46**, 7849–7852; (d) S. O. Kang, J. M. Llinares, V. W. Day and K. Bowman-James, *Chem. Soc. Rev.* 2010, **39**, 3980–4003; (e) R. Hu, J. Feng, D. H. Hu, S. Q. Wang, S. Y. Li, Y. Li and G. Q. Yang, *Angew. Chem., Int. Ed.* 2010, **49**, 4915–4918; (f) J. Yoon, S. Kim, N. J. Singh and K. S. Kim, *Chem. Soc. Rev.* 2006, **35**, 355–360; (g) D. Buccella, J. A. Horowitz and S. J. Lippard, *J. Am. Chem. Soc.* 2011, **133**, 4101–4114; (h) Z. C. Xu, K. H. Baek, H. N. Kim, J. N. Cui, X. H. Qian, D. R. Spring, I. Shin and J. Y. Yoon, *J. Am. Chem. Soc.* 2010, **132**, 601–610; (i) L. Xue, G. P. Li, D. J. Zhu, Q. Liu and H. Jiang, *Inorg. Chem.* 2012, **51**, 10842–10849; (j) Z. J. Guo, *Coord. Chem. Rev.* 2004, **248**, 205–229; (k) Y. Li, Q. Zhao, H. Yang, S. Liu, X. Liu, Y. Zhang, T. Hu, J. Chen, Z. Chang and X. Bu, *Analyst.* 2013, **138**, 5486–5494.

12. A. Liu, L. Yang, Z. Zhang, Z. Zhang and D. Xu, *Dyes Pigm.*, 2013, **99**, 472–479.
13. Q.-F. Hou, L. Ye and S.-M. Jiang, *Acta Cryst.*, 2007, **E63**, o939–o940.
14. Y. Diskin-Posner, G.K. Patra and I. Goldberg, *J. Chem. Soc. Dalton Trans.*, 2001, 2775.
15. T. Moriuchi, S. Bandoh, M. Kamikawa and T. Hirao, *Chem. Lett.*, 2000, **29**, 148.
16. K. Smolarek, L. Bujak, S. Mackowski, and E. Schab-Balcerzak, *J. Phys. Chem. A*, 2013, **117**, 10320–10332.
17. R. K. Pathak, V. K. Hinge, A. Rai, D. Panda and C. P. Rao, *Inorg. Chem.*, 2012, **51**, 4994.
18. (a) T. Han, X. Feng, B. Tong, J. Shi, L. Chen, J. Zhi and Y. Dong, *Chem. Commun.*, 2012, **48**, 416–418; (b) N. E. W. Alstad, B. M. Kjelsberg, L. A. Vøllestad, E. Lydersen and A. B. S. Poléo, *Environ. Pollut.*, 2005, 133, 333–342; (c) S. Das, A. Sahana, A. Banerjee, S. Lohar, D. A. Safin, M. G. Babashkina, M. Bolte, Y. Garcia, I. Hauli, S. K. Mukhopadhyay and D. Das, *Dalton Trans.*, 2013, **42**, 4757–4763.
19. (a) K. C. Song, H. Kim, K. M. Lee, Y. S. Lee, Y. Do and M. H. Lee, *Sens. Actuators, B*, 2013, **176**, 850–857; (b) S. Maruyama, K. Kikuchi, T. Hirano, Y. Urano, T. Nagano and A. Novel, *J. Am. Chem. Soc.*, 2002, **124**, 10650–10651. (c) A. P. Silva, H. Q. N. Gunaratne, T. Gunnlaugsson, A. J. M. Huxley, C. P. McCoy, J. T. Rademacher and T. E. Rice, *Chem. Rev.*, 1997, **97**, 1515–1566.
20. (a) H.M. Park, B.N. Oh, J.H. Kim, W. Qiong, I.H. Hwang, K.-D. Jung, C. Kim and J. Kim, *Tetrahedron Lett.*, 2011, **52**, 5581–5584; (b) D. Maity and T. Govindaraju, *Eur. J. Inorg. Chem.*, 2011, **36**, 5479–5485; (c) W.-H. Ding, W. Cao, X.-J. Zheng, D.-C. Fang, W.-T. Wong and L.-P. Jin, *Inorg. Chem.* 2013, **52**, 7320–7322; (d) S.J. Kim, J.Y. Noh, K.Y. Kim, J.H. Kim, H.K. Kang, S.W. Nam, S.H. Kim, S.S. Park, C. Kim and J.H. Kim, *Inorg. Chem.* 2012, **51**, 3597–3602.

GRAPHICAL ABSTRACT

A reversible fluorescent-colorimetric imino-pyridyl bis-Schiff base sensor for expeditious detection of Al^{3+} and HSO_3^- in aqueous media

Anupam Ghorai, Jahangir Mondal, Rukmani Chandra and Goutam K Patra*

Department of Chemistry, Guru Ghasidas Vishwavidyalaya, Bilaspur (C.G)

A reversible fluorescent-colorimetric imino-pyridyl bis-Schiff base receptor (N^1E, N^4E)- N^1, N^4 -bis(pyridine-4-ylmethylene)benzene-1,4-diamine (**L**) for easy, convenient, rapid and sensitive detection of both Al^{3+} and HSO_3^- in aqueous medium has been developed. The receptor **L** shows remarkable detection ability in a wide pH range of 4–11 and successfully utilised in the determination of Al^{3+} in aqueous solution of bovine serum albumin protein and HSO_3^- in real food samples.

